Remote Sensing of Environment 126 (2012) 174–183

Contents lists available at SciVerse ScienceDirect

Remote Sensing of Environment

journal homepage: www.elsevier.com/locate/rse

Global phenological response to climate change in crop areas using satellite remote sensing of vegetation, humidity and temperature over 26 years

M.E. Brown [a,*], K.M. de Beurs [b], M. Marshall [c]

[a] Biospheric Sciences Branch, Code 614.4, NASA Goddard Space Flight Center, Greenbelt, MD 20171, USA
[b] Department of Geography and Environmental Sustainability, The University of Oklahoma, Norman, OK, USA
[c] Department of Geography, University of California Santa Barbara, Santa Barbara CA, USA

ARTICLE INFO

Article history:
Received 30 March 2012
Received in revised form 6 August 2012
Accepted 11 August 2012
Available online 11 September 2012

Keywords:
Phenology
NDVI
Agriculture
Cereal crops
Temperature
Humidity

ABSTRACT

The recent increase in food prices has revealed that climate, combined with an expanding population and a widespread change in diet, may result in an end to an era of predictable abundance of global cereal crops. The objective of this paper is to estimate changes of agriculturally-relevant growing season parameters, including the start of the season, length of the growing period and the position of the height or peak of the season, in the primary regions with rainfed agriculture during the past 26 years. Our analysis found that globally, 27% of cereal crop areas have experienced changes in the length of the growing season since 1981, the majority of which had seasons that were at least 2.3 days per year longer on average. We also found both negative and positive trends in the start of season globally, with different effects of changing temperature and humidity being isolated depending on the country and region. We investigated the correlation between the peak timing of the growing season and agricultural production statistics for rain fed agriculture. We found that two thirds of the countries investigated had at least 25% of pixels with crop production that behaved differently than expected from the null hypothesis of no correlation. The results show that variations in the peak of the growing season have a strong effect on global food production in these countries. We show that northern hemisphere countries and states appear to have improved model fit when using phenological models based on humidity while southern hemisphere countries and states have improved model fit by phenological models based on accumulated growing degree days, showing the impact of climate variability during the past two and a half decades.

Published by Elsevier Inc.

1. Introduction

In the next two decades, the demand for food will double, necessitating significant investments in production (IAASTD, 2008). Agricultural productivity has greatly increased in the past through improvement of yields in many regions and expansion of cropped area in lesser-developed areas. Research during the past decade has documented changes in climate and land-atmosphere response that may affect agriculture (IPCC, 2007). These include increasing temperatures, changing precipitation regimes and shifting seasonal cycles. Tropical agricultural systems are particularly sensitive to changes in evapotranspiration and movement of the monsoon (Zhao & Running, 2010). How global environmental change will affect the productivity of global agricultural systems and the ability of farmers to adapt to changing moisture availability patterns is still uncertain, particularly in regions with fewer resources to invest in change.

Previous research has shown the impact of temperature variability on agricultural regions both in temperate regions (de Beurs & Henebry, 2004) and tropical regions (Liebmann & Marengo, 2001; Piao et al., 2007). Vegetation data from the AVHRR series of satellites has been used to investigate trends through time (Nemani et al., 2003), and results have shown a difference between the 1980s-1990s and the 2000s (Piao et al., 2003; Zhao & Running, 2010), which was postulated to be due to a widespread decline in moisture availability.

Rainfed agriculture is sensitive to variations in water availability, resulting in variations in overall production over large areas (Jeong et al., 2010; Simelton et al., 2009). The impact on agriculture of increased evapotranspiration and changes in plant growth due to increasing temperatures is not yet known, although many studies have postulated widespread effects on primary productivity across biomes (Graaff et al., 2006; Nemani et al., 2003). Changes in local productivity will negatively affect global food security, since most of the developing world relies on local food production and most food is consumed locally without ever reaching the international marketplace (Lamb, 2000; Schmidhuber & Tubiello, 2007). Increasing disparity in purchasing power among nations will heighten the importance of local production, making it increasingly critical that we understand

* Corresponding author. Tel.: +1 301 614 6616.
E-mail address: molly.brown@nasa.gov (M.E. Brown).

0034-4257/$ – see front matter. Published by Elsevier Inc.
http://dx.doi.org/10.1016/j.rse.2012.08.009

how changes in seasonality influence agricultural productivity (Brown et al., 2009; Funk & Brown, 2009).

The objective of this paper is to estimate changes of agriculturally-relevant growing season parameters, including the start of the season, length of the growing period and the position of the height or peak of the season, in the primary regions with rainfed agriculture during the past 26 years. Our focus here is to determine if it was moisture or temperature conditions that are most related to agricultural production variations, as this question is a central one for projecting the impact of climate change on food production (Lobell et al., 2011). This paper uses the satellite remote sensing observational record to identify the impacts of climate change on growing season phenology in cropped areas. Through an interrogation of start of season, peak timing and length of growing season globally, we identify locations where change has occurred. By correlating observed agricultural production and peak timing derived by four versions of our phenology models, we can determine the most powerful and explanatory metrics that help us locate the cropping regions that are most sensitive to weather variability.

2. Materials and methods

We used the AVHRR NDVI dataset from the NASA Global Inventory Monitoring and Modeling Systems (GIMMS) group at the Laboratory for Terrestrial Physics (Tucker et al., 2005). The dataset contains 15-day maximum value NDVI composites at 8-km resolution for July 1981 to December 2006. It is based on six NOAA (National Oceanic and Atmospheric Administration) satellites (Kidwell, 1998, 2000). SPOT Vegetation NDVI is used for intercalibration between the AVHRR/2 and AVHRR/3 series of the sensors. The GIMMS dataset is corrected for factors not relating to vegetation, although some data problems remain in the current version (Brown et al., 2006). Due to AVHRR's wide spectral bands the presence of water vapor in the atmosphere lowers NDVI values, although maximum value compositing reduces this effect (Holben, 1986). We regridded the GIMMS data from its native Albers equal area 8 km resolution to 0.08 degree resolution to make it fit better with the weather data.

We used accumulated growing degree days (AGDD) and humidity data derived from the Global Land Data Assimilation System (GLDAS) (Fang, 2009) in the growing season analysis (Kumar et al., 2006). The GLDAS dataset used in this study consists of 3-hourly gridded meteorological data used to drive global land surface models at one degree from 1979 to 2009. The dataset is synthesized across the time series by assimilating various ground-based, remote sensing, and surface climate reanalysis data (Berg et al., 2003; Idso, 1981; Shapiro, 1987) from 2000 to 2009. We regridded the GDD and humidity data from the native resolution of 1 degree to 0.08 degree and aggregated the 3-hourly product to daily. The 3-hourly temperature and relative humidity data were averaged over the day. GDD was computed by subtracting the base temperature (5 C) from average daily temperature. If the average daily temperature fell below the base temperature, it was not included in the summation. Daily average GDD and relative humidity were then summed over the 18 month period to create AGDD and accumulated relative humidity (Arhum).

The location of crops globally was estimated using the Monfreda harvested area and yields data created by combining national, state, and county level census statistics with a recently updated global data set of croplands on a 5 min by 5 min (~10 km by 10 km) latitude–longitude grid (Monfreda et al., 2008). The resulting land use data sets depict year 2000 area harvested and yield of 175 distinct crops of the world. We used all the aggregated crop maps to produce a single map of the location of all major rainfed crop groups, including annuals/perennials, herbaceous/shrubs/trees, C3/C4, and leguminous/ nonleguminous. We gridded the cereal crop product to 0.08 degree to create a mask of where rainfed crops can be found globally, excluding non-agriculture areas from the analysis (Fig. 1).

2.1. Agricultural production statistics

We used the annual rainfed cereal production estimates from 1982 to 2006 from the United Nation's Food and Agriculture Organization (FAO) as statistics to enable an analysis of the impact of phenological variations on production at the country-level (FAO, 2011). Although country-level cereal statistics are not at an optimal resolution, these production statistics are the most reliable, comparable and comprehensive information on agriculture available.

For the United States we used wheat survey data from 1982 to 2006 from the US Department of Agriculture's National Statistics Service (NASS) (NASS, 2012). We use the wheat information because it extends back to the 1980s and provides information on rainfed agriculture. For Europe, we use the FAO cereals data by country, but create four regions since many of the countries in Europe are very small (Fig. 2). This enables an improved estimation of the significance of the results.

2.2. Methods

This paper is based on extensive previous research using vegetation index observations as the basis for measurements of phenological metrics (de Beurs & Henebry, 2008). Here we first estimate the start of the growing season based on NDVI with the midpoint pixel method (White et al., 1997; White et al., 2009). Subsequently, we use the quadratic method with either Arhum or AGDD as dependent variable to characterize the remainder of the growing season (de Beurs & Henebry, 2010) Fig. 3 shows the general scheme of the models. Previously we have shown that quadratic models linking NDVI with AGDD fit well for land surface phenology in temperate climates with agricultural or herbaceous vegetation (de Beurs & Henebry, 2004). We have demonstrated that the quadratic models also work in rainfed agricultural areas (Brown & de Beurs, 2008). The quadratic regression models can be applied directly to the data without the need of applying filters to remove noisy data. The basic quadratic regression model is given as:

$$\mathrm{NDVI} = \alpha + \beta x + \gamma x^2$$

Where, x, is either AGDD or Arhum. The slope parameter (β) and the quadratic parameter (γ) together determine the green-up period, defined as the amount of accumulated relative humidity (%) or accumulated growing degree days (AGDD) necessary to reach the peak NDVI. The peak NDVI itself can be determined based on the peak position.

We applied the quadratic model to 26 years of NDVI data with an adjusted modeling strategy to account for both monsoonal systems where the temperature is fairly constant and growing season onset is driven by rainfall and those that are controlled by temperature. We first applied the midpoint pixel method that has been demonstrated to provide the start of season (SOS) and end of season (EOS) observations closest to field measurements over North America in a large scale comparison study (White et al., 2009). We are not aware of any studies that have specifically compared the performance of different land surface phenology methods over croplands. While the White et al. (2009) comparison study did not specifically investigate the accuracy of SOS and EOS measures over croplands, the midpoint pixel method was shown to be one of the most consistent methods for the estimation of SOS over a variety of ecosystems. In the second step we fit the quadratic model for the growing season, which is determined by SOS and EOS. The quadratic model estimates the peak height (NDVI) and peak position (AGDD or Arhum). We also report the model fit (R^2_{adj}), which gives an indication of how well our

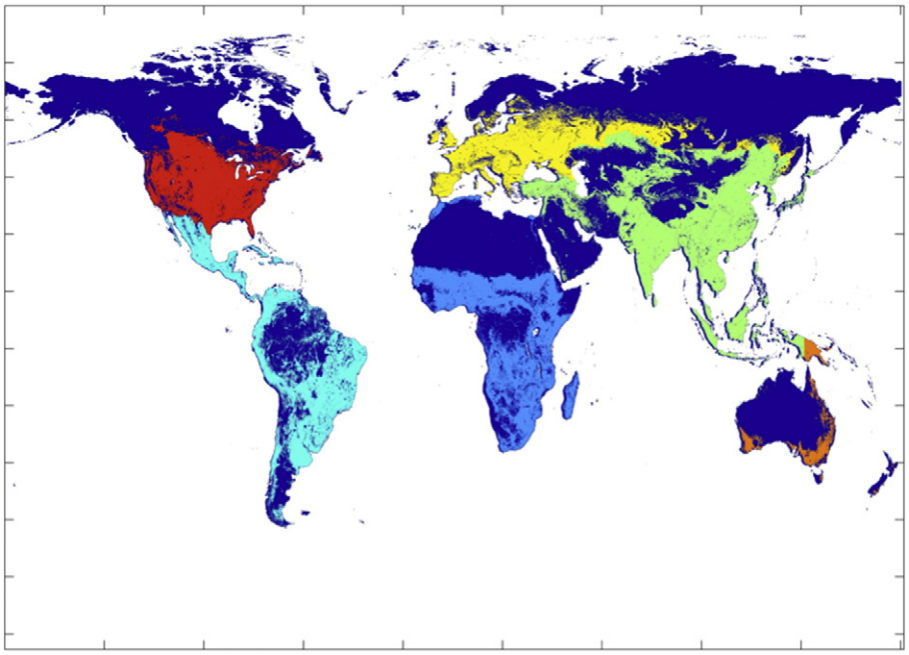

Fig. 1. Map showing the cropland areas taking into consideration. Yellow areas are cropped and grey are non-cropped. Data adapted from Monfreda et al. (2008).

quadratic models fit. Sudden changes in R^2_{adj} could indicate disturbances. Based on the SOS and EOS we also calculate the length of the growing season. As in previous work, we run the model for a period of 18 months so that all growing dynamics can be captured (Brown et al., 2010). Thus we have four model outputs for each location: relative humidity (Arhum)-NDVI model and the AGDD-NDVI model for both cycle 1 (the18-month period from October through March of the following year) and cycle 2 (the 18-month period from April through September of the following year). For a longer description of the phenology model, please see de Beurs and Henebry (2008) and Brown et al. (2010).

2.3. Statistical analysis

We used the 24 years of phenology metrics to calculate interannual variation and temporal trends in the start of season, peak period and length of growing season in the global crop areas by pixel. The timings of these parameters were calculated to the day because we take the day of the satellite observation into account. Correlation coefficients and significance tests are used to estimate changes over the period of analysis, 1982 to 2006.

We use AGDD and Arhum to peak to test the ability of phenology models to capture interannual variations of agricultural production.

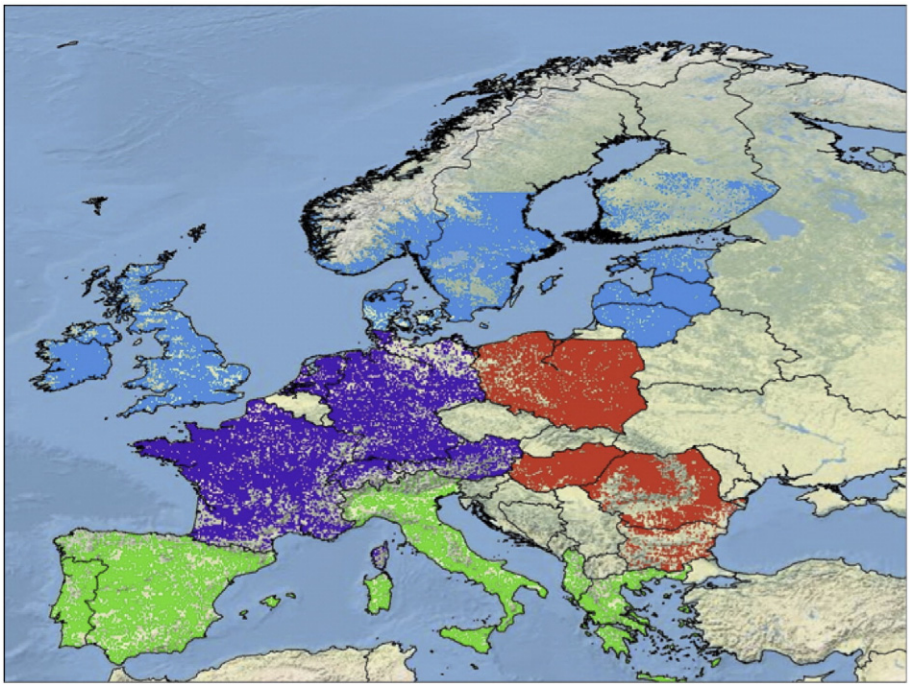

Fig. 2. Map showing the delineation of the European countries into four regions. Purple areas are western Europe, green are southern Europe, red are eastern Europe and blue are northern Europe.

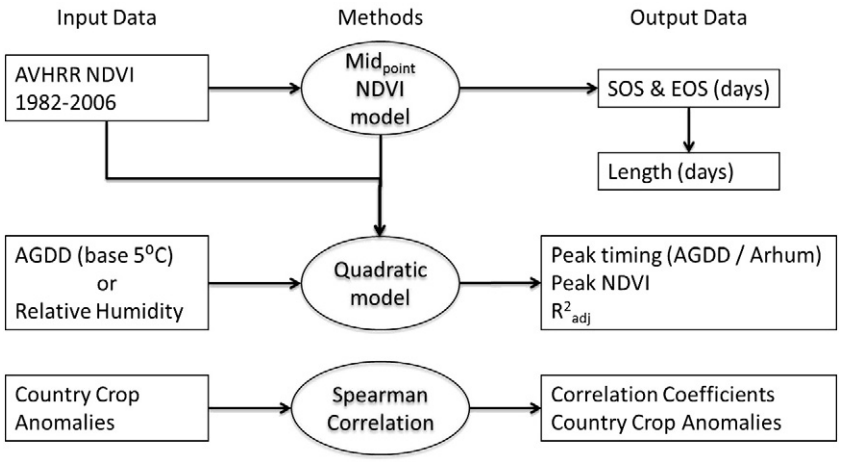

Fig. 3. Flow diagram showing how NDVI, humidity and temperature data were used to analyze how seasonality changes have agriculture over the past 26 years.

By deriving spearman rank correlations between production anomalies and annual metrics of seasonality, we identified regions whose agricultural production was most susceptible to variations in the weather as observed by variability in land surface phenology during the 1982–2006 period. Since we are studying a very large number of pixels, we have a high probability of finding a certain number of false positives. Consider this example. Were we interested in only a single pixel for which the null hypothesis was true, then the chance that we would find a correlation with a p-value lower than 0.01 is very small (<1%). Under the null hypothesis of no correlation, the distribution of p-values from a large number of Spearman correlation tests is uniform over the interval [0,1]. Thus, if an α level of 0.1 is chosen as a cutoff, for any given experiment, one of ten p-values could be 0.1 or less, even when the null hypothesis is true (Hung et al., 1997). If we perform a correlation test for 100 independent pixels for which the null hypothesis is true, then the chance that we will find at least one pixel with a significant correlation ($p<0.1$), can be calculated as one minus the chance that there are no significant correlations.

Bonferroni correction and other classical methods to control the family-wise error rate are too conservative when investigating thousands of correlations which are spatially correlated (Brown et al., 2010). New methods, such as the false discovery rate, have been developed to control error rates for those studies with thousands of samples that are less stringent than the family-wise error rates. In a previous study we have shown that the false discovery rate and p_0 values (Brown et al., 2010; Storey & Tibshirani, 2003) can be beneficial to better understand the results of satellite image analysis. Here we follow a similar approach and calculate $1-p_0$, with p_0 defined as the overall proportion of true null features (pixels lacking correlation/total number of pixels). The p_0 is derived from the p-value distribution. The value $1-p_0$ presents the proportion of pixels that behaved differently than expected from the null hypothesis (Storey & Tibshirani, 2003). We compare four different peak timing variables (based on AGDD and Arhum for cycle 1 and cycle 2) with available production statistics per country. We report the model with the highest $1-p_0$ value, indicating the proportion of pixels that reveal correlation, for each country, state or region. In this way we were able to characterize how widespread the correlation between production and the peak timing of the growing season was.

3. Results

Fig. 4 shows overall results from the analysis. The model skill in Fig. 4A is the mean of the correlation coefficient for all 26 years from the accumulated humidity (Arhum) model runs. Fig. 4B shows the correlation coefficients for the accumulated growing degree days (AGGD5). The models show high degree of skill in predicting the NDVI seasonal curve across years in North America, Eurasia and Africa. South America and tropical south Asia overall have lower R^2 statistics, possibly due to clouds and the use of AVHRR data with a less effective cloud screen than is optimal (Tucker et al., 2005). Tropical regions typically have a much weaker seasonal signal as they are green throughout the year, thus these lower correlations are to be expected.

Fig. 4C shows the mean length of the growing season in calendar days for all years, revealing longer growing seasons in the tropical regions of Africa, Asia and South America, as well as in the eastern regions of the United States. Fig. 4D shows the mean start of season, which is later in tropical regions in the northern hemisphere and earlier in temperature-controlled regions. Throughout the paper, we report only one length and start of season result because these parameters are estimated using NDVI alone, before the model is fit using humidity and temperature (see Fig. 3).

Fig. 4E,F shows the model-derived peak position of the growing period. The model is tuned using humidity and growing degree-days, yielding different results. Fig. 4E is expressed as accumulated % humidity and shows the later peak in the low latitude-tropics, and an earlier peak in the dry mid-latitude northern regions such as in southeast Asia and the American west. Fig. 4F is expressed in the number of growing degree-days, thus results in the thousands in tropical ecosystems are expected.

3.1. Trends in seasonal parameters

Fig. 5 shows the trends in the start and length of the growing season through the 26 years. There are a fairly equal number of positive and negative trends seen, with regions experiencing earlier start of the growing season shown in blue and red for later start of the season. Fig. 5A shows the West African Sahel has been experiencing a later growing season start, along with southeast Asia and North America. Droughts and colder springs in the 1980s explain these trends (Hicke et al., 2002; Jarlan et al., 2005; Nicholson, 2005; Zhou et al., 2003). Europe generally reveals an earlier start of the growing season which can be partly explained by large scale atmospheric oscillations (de Beurs & Henebry, 2008).

For the length results (Fig. 5B), positive regression results (red) mean a longer growing period over the 26 years and negative regression results (blue) means shorter growing seasons through time. Our

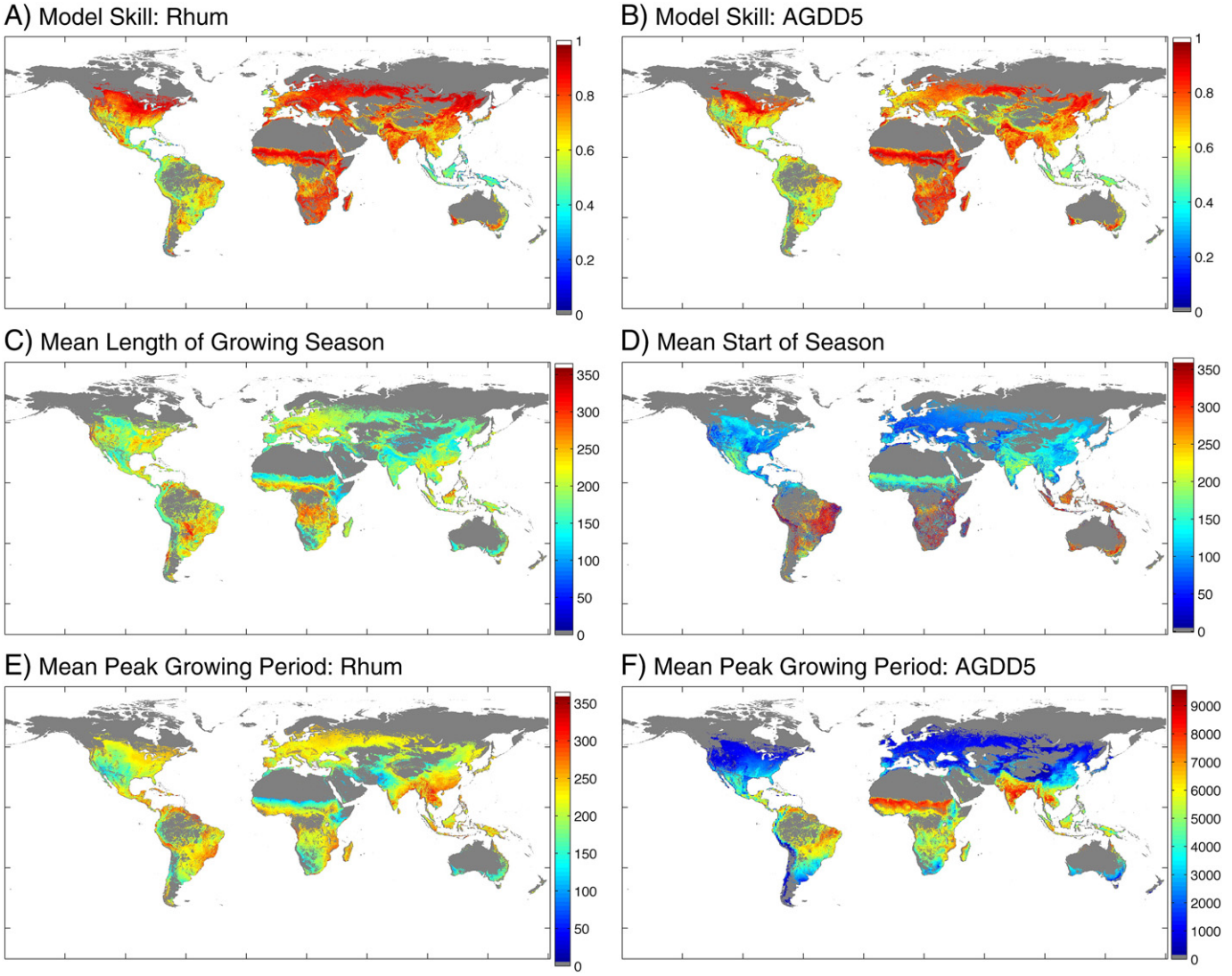

Fig. 4. Summary of results. Top row shows the temporal mean of the coefficient of determination of the phenology model (R^2_{adj}) for A. accumulated humidity (Arhum) and B. growing degree days (AGDD5). Second row shows the average start of the season by pixel over the 26 years (C) and the average length of the season in julian days (D). Bottom row shows the peak period for accumulated humidity model in accumulated % humidity (E) and the accumulated temperature model in degrees Celsius over the season (F).

analysis found that globally, 27% of cereal crop areas have experienced changes in the length of the growing season since 1982, the majority of which had seasons that were 2.3 days per year longer on average. Agricultural areas in Europe clearly reveal an earlier start of the season and a longer growing period. Northern North America crop areas have the opposite trend, with later starts and shorter growing seasons according to this model. Regions in the Sahel in northern Africa have a shorter growing period through time, a trend that can be seen also in northern India and in south Asia. Australian crop regions show both an earlier start and a shorter length overall, due to the highly variable climate seen in the region.

Fig. 6 shows the trends in the peak growing period timing. This figure shows overall positive trends in the peak timing, meaning they are shifting from lower accumulated humidity and growing degree days to peaks at higher humidity and growing degree days in the northern hemisphere. These trends are particularly strong in the model tuned with relative humidity, with strong signals in Eastern Europe and in the eastern United States. Negative trends in peak timing can be seen in dry regions of south Asia, in India and in the arid southwest in North and South America. Very strong positive trends are seen in the peak timing of the accumulated growing degree-day model (AGGD5) in Asia, with later peaks being experienced in the northern cropping regions in the Eastern hemisphere.

3.2. Correlations with production

To understand the impact of changes in phenology seen in the models, we correlated the anomaly of the peak growing season position for all cropped pixels with the annual production from each country's United Nations statistics.

Fig. 7 shows the time series from ten selected countries with high overall correlations with production anomalies. The plot shows that some regions have positive changes and others negative, showing that the variability of peak position captures production anomalies quite well in some regions. The more developed agricultural regions such as Germany also have fairly high correlation series.

In total we analyzed the correlation between production and the peak timing derived from four models for 114 countries around the world (Fig. 8A). We have removed the United States from this list because we will discuss the states separately below. We found 75

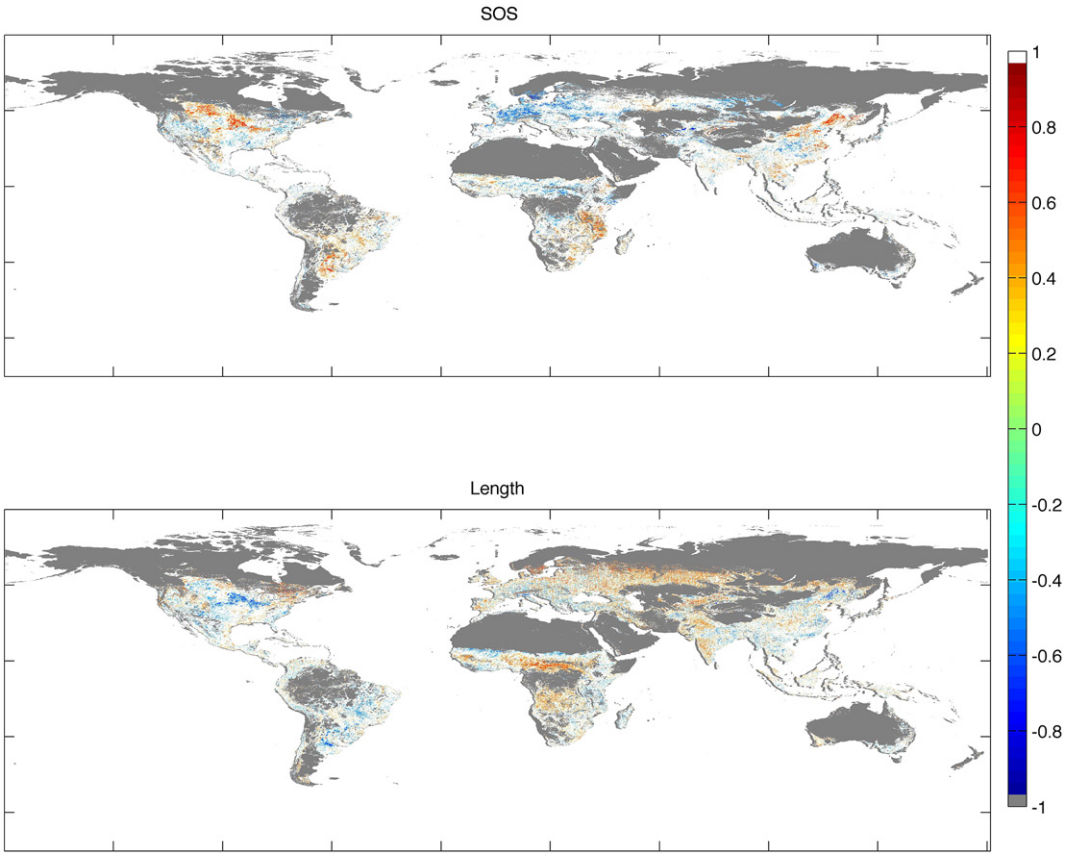

Fig. 5. Significant trends of Start of Season (top) and length of growing season (bottom) over the 26 years in cropping regions, given by the regression coefficient of the parameter vs time. Significance is measured by *p* value of less than 0.1.

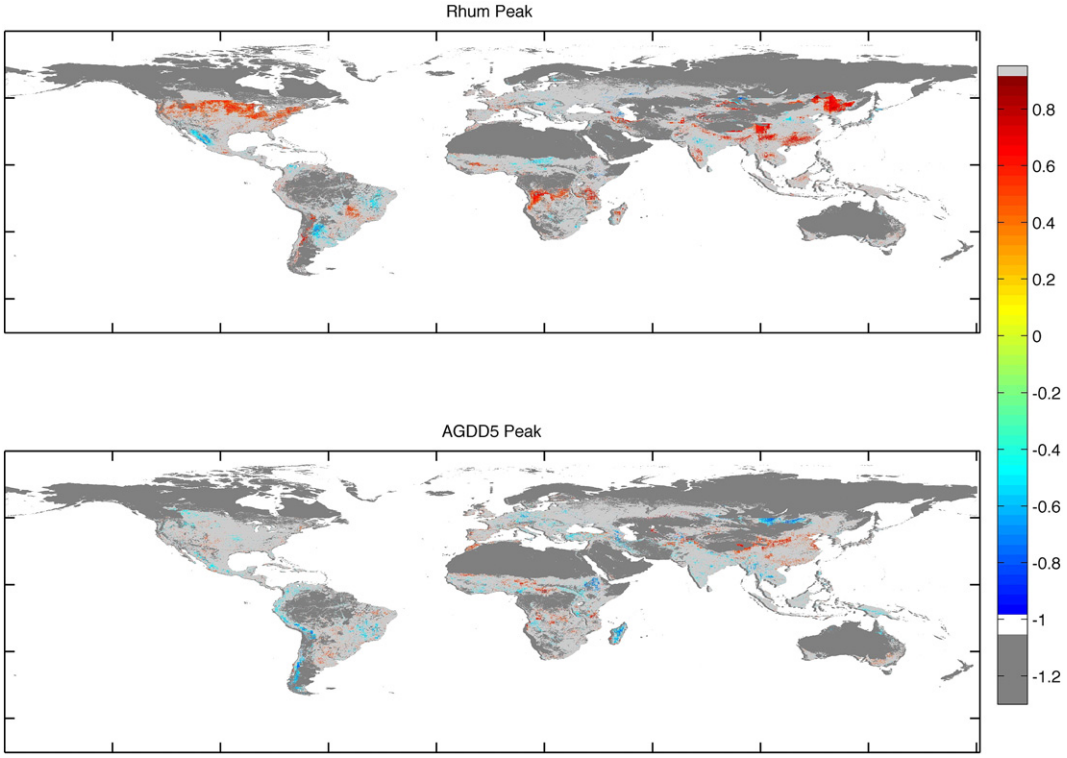

Fig. 6. Significant trends of peak period for relative humidity model (top) and accumulated growing degree-days (bottom) for 26 years in cropping regions, given by the regression coefficient of the parameter vs time. Significance is measured by *p* value of less than 0.1.

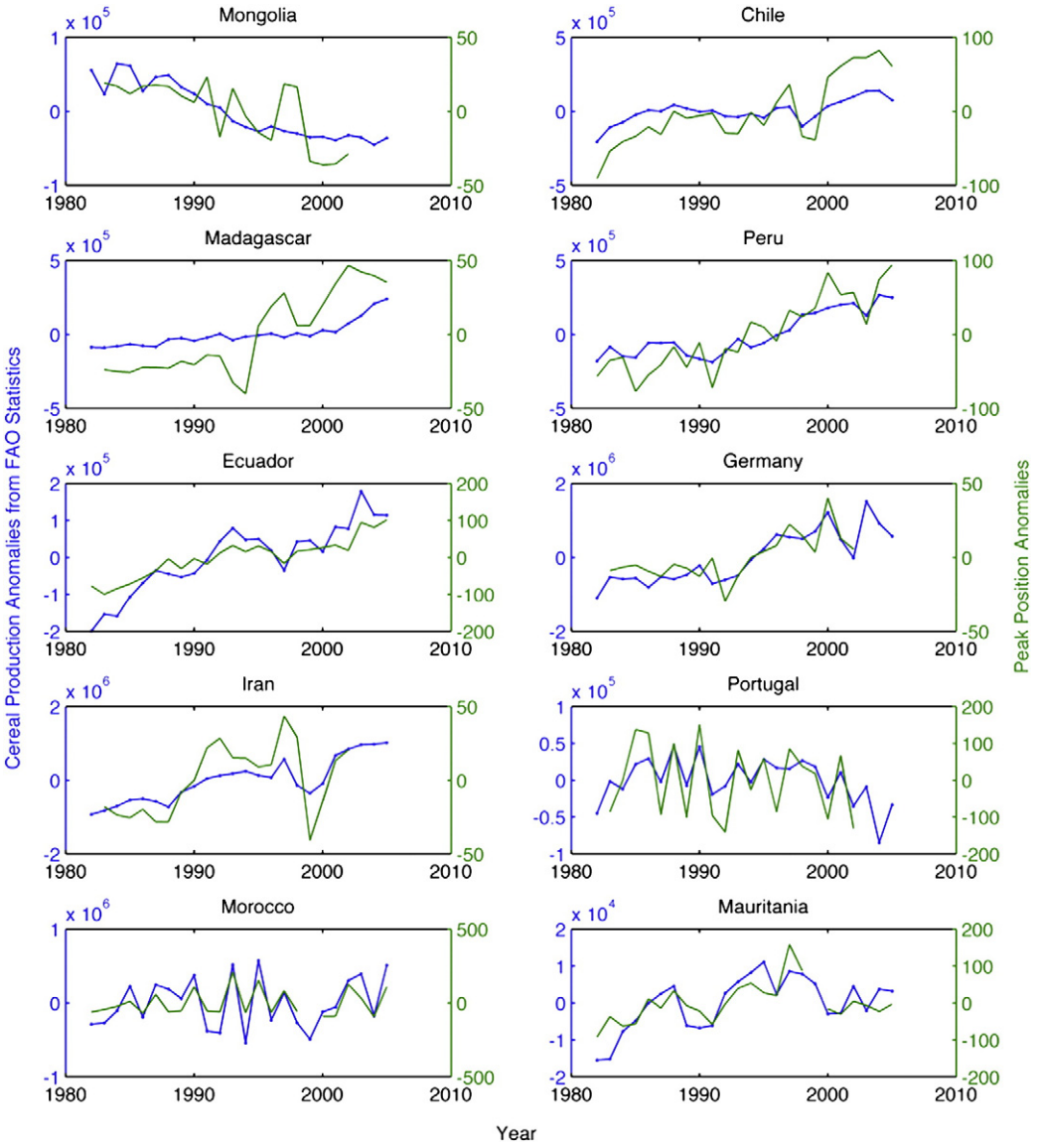

Fig. 7. Time series of production anomalies and peak position from the Humidity model are derived by selecting only the pixels with a correlation coefficient of over 0.6 for the annual mean displayed. Ten countries are displayed in this figure, with cereal production anomalies (blue dot) and peak position anomalies (green line).

countries for which at least 25% of the pixels behaved differently than expected from the null hypothesis of no correlation (Fig. 8B). A total of 17 of these countries are located in Europe. The majority of the remaining countries (57) have best fitting models for cycle 1(42 of the countries). These countries are predominantly located the Northern Hemisphere although Namibia and South Africa also fell in this group. We found that for cycle 1 there were 20 countries that had model outputs that best correlated with production based on AGDD and 22 that had model outputs that best correlated with country production based on Arhum. We found only five countries (Philippines, Libya, Rwanda, Peru and Ecuador) that had model outputs based on AGDD that best correlated with production statistics in cycle 2 and 10 countries that had model outputs that best correlated with production statistics based on Arhum in cycle 2 (Fig. 8B). The last group was predominantly located in Southern Africa, with the exception of Argentina and Egypt. Note that we have omitted the countries of the former Soviet Union because we did not have the full production statistics available per country before 1991.

3.3. Results for the United States

Table 1 gives the 1-p_0 values for the fifteen states with the largest average wheat production totals in the United States. It is important to remember that we are only investigating rainfed agriculture. Thus, the large wheat areas of Kansas, Oklahoma and Texas that are irrigated by water from the Ogallala aquifer are not taken into consideration. Of the 15 states, 13 revealed pixels that behaved differently than would be expected under the null hypothesis of no correlation. Only Minnesota and Ohio did not reveal significant behavior. The remaining states revealed 1-p_0 values ranging from as high 0.99 in North Dakota, indicating that almost all pixels reveal behavior according to significant correlation, to 0.11 for Oregon where just 11% of the pixels revealed significant correlation behavior. All states, except Washington and Idaho, revealed the most significant pixels for cycle 1. The states reveal a mixture of model preferences with the model based on AGDD resulting in the most significant pixels in the more southern states: Kansas, Oklahoma, Texas, Colorado, Nebraska,

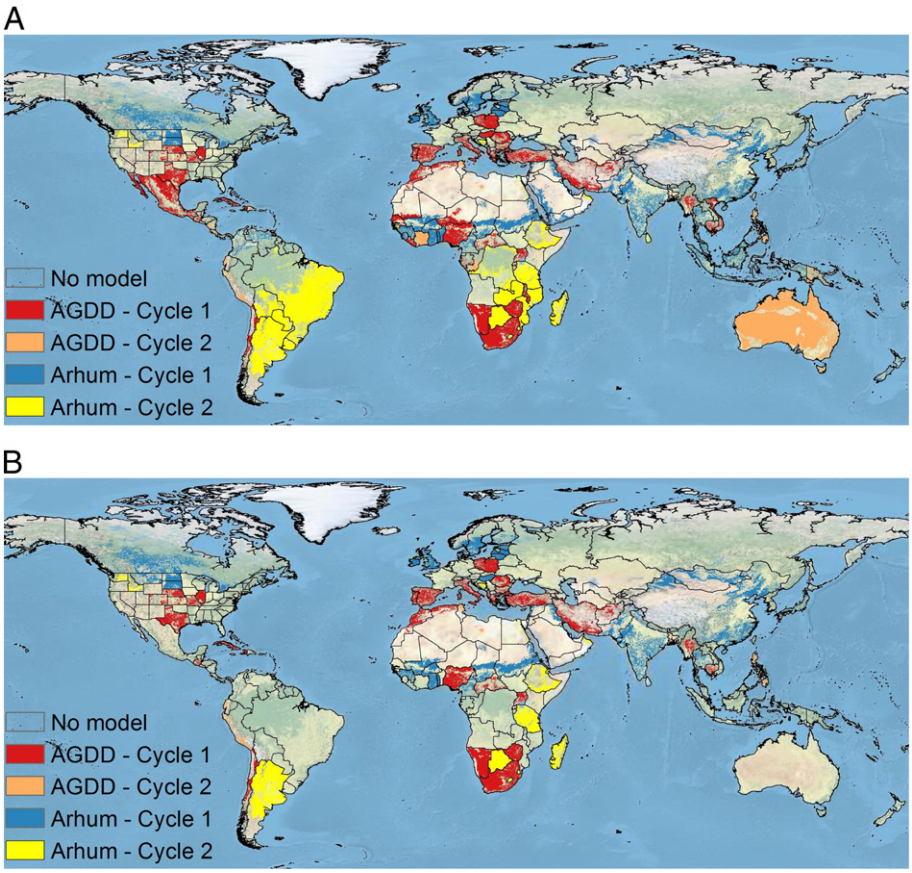

Fig. 8. Top: overview map showing which model results in phenological metrics that best correlate with production statistics. For each cropland pixel in each country/state or region the model type is shown that reveals the most correlated pixels with production. Countries that were part of the former Soviet Union and countries that were part of former Yugoslavia are omitted. Countries that do not reveal a significant model are omitted as well. Bottom: same as above but only the countries for which at least 25% of the pixels show a significant behavior are show.

Illinois and Missouri. The remaining states, North and South Dakota, Washington, Montana, Idaho and Oregon revealed the largest number of significant pixels when the humidity based models were applied.

3.4. Results for Europe

Fig. 2 gives the croplands in the four regions in Europe that we investigated. Note that we do not have data for Belgium and Luxemburg.

Table 1
The $1-p_0$ values for the fifteen states with the largest average wheat production totals in the United States. The states are ordered by $1-p_0$ value.

State	$1-p_0$	Model
North Dakota	0.9986	Arhum, cycle 1
Montana	0.8701	Arhum, cycle 1
Missouri	0.8657	AGDD, cycle 1
Nebraska	0.7087	AGDD, cycle 1
Washington	0.6815	Arhum, cycle 2
Kansas	0.6718	AGDD, cycle 1
Illinois	0.6438	AGDD, cycle 1
Colorado	0.5182	AGDD, cycle 1
Idaho	0.3488	Arhum, cycle 2
South Dakota	0.3095	Arhum, cycle 1
Texas	0.3054	AGDD, cycle 1
Oklahoma	0.1970	AGDD, cycle 1
Oregon	0.1123	Arhum, cycle 1
Minnesota	0	N/A
Ohio	0	N/A

We also do not investigate Czech Republic and Slovakia or the countries making up former Yugoslavia since we do not have continuous time series for these areas.

Only Western Europe does not reveal significant correlation between peak timing and production statistics (Table 2). When the countries in this region were investigated separately we did find significant behavior in Germany ($1-p_0=0.53$) and France ($1-p_0=0.38$). More than 50% of the pixels in Northern and Southern Europe reveal behavior consistent with significant correlation. It is interesting to note that northern Europe reveals the most correlation with production for models based on relative humidity while southern Europe reveals the most correlation with production for models based on AGDD. These differences appear consistent with what we find for the United States, where the production in Northern states typically had better correlations with AGDD while the production in Southern states had better correlations with Arhum.

Table 2
The $1-p_0$ values for the four regions delineated in Europe. The regions are ordered by $1-p_0$ value.

Region	$1-p_0$	Model
Northern Europe	0.5101	Arhum, cycle 1
Southern Europe	0.5086	AGDD, cycle 1
Eastern Europe	0.2249	AGDD, cycle 1
Western Europe	0.0011	Arhum, cycle 1

4. Discussion

Research has shown that in the 1980s and 1990s, climate change has manifested in a warming of the northern hemisphere and a subsequent lengthening of the growing period in many regions (Nemani et al., 2003; Slayback et al., 2003). Biological productivity gains seen in these decades did not continue in the 2000s, however, due to widespread drought and reductions in moisture availability (Piao et al., 2006). Many of these analyses have been conducted using phenology models using satellite remote sensing of vegetation also used in our study (White et al., 2009). Phenology models have the advantage of being more robust and easier to validate than the vegetation index alone (Brown & de Beurs, 2008).

The results shown here demonstrate the increasing importance of moisture conditions necessary for crops and other vegetation to take advantage of higher temperatures and longer growing seasons. Moisture availability is a primary constraint to productivity in regions experiencing rapid warming and thus increased evapotranspiration during the peak of the growing season. Agricultural activities are significantly affected by variations in rainfall, thus including humidity in the phenology model clearly improves the ability of the model to capture changes in production. Significant correlations between the peak position measured in growing degree-days or relative humidity with rainfed cereal production demonstrates the continued vulnerability of the agricultural system to local climate. As the impact of climate change continues to be felt in growing areas around the world, increased volatility in food production should be expected.

The peak metric combines both the timing of the growing season and its response to temperature and moisture availability, improving the ability of phenological models to capture the differential effect of climate on the larger agricultural system. We have previously shown that the peak metric captures the overall growing season better than the start of season estimation, which typically displays a lot of variability due to snow and other non-vegetation related issues (de Beurs & Henebry, 2008, 2010). The start of the growing season is also likely less sensitive to overall food production.

Recent increases in global commodity prices has revealed that climate, combined with an expanding population and a widespread change in diet, may result in an end to an era of predictable abundance of global cereal crops. After a series of floods and droughts, food production in 2011 is not keeping up with demand. Growing conditions in diverse agricultural systems can be observed using the start, length and peak period of the growing season in the cereal producing regions of the world since 1982. Our analysis shows that during the past two decades, climate has had a significant impact on food production, which is likely to become increasingly important as temperatures and moisture conditions change.

There are significant limitations to this research. Due to the coarse scale of the AVHRR data, the analysis only has limited utility at the farm scale. AVHRR data has a native resolution of 8 km, and through the 1981–2008 record, has a one pixel error (Tucker et al., 2005). Thus trends in soil degradation or use of chemical fertilizer at a scale of one or many farms will not show up in this analysis. The humidity and temperature data used in this analysis are modeled, thus incorporating all the model errors in the GLDAS data assimilation system. The country-level statistics are far from optimal. Sub-national statistics such as those available in the United States for very large countries such as Brazil, Sudan, and China would greatly improve the results.

5. Conclusions

The most interesting results from this analysis show the increasing importance of temperature for affecting production statistics. This has been seen in regions such as Zimbabwe and Kenya through the crop analysis work of the Famine Early Warning Systems Network (Funk et al., 2008). Here we have documented at the global scale countries that have seen the effects of trends in temperature on agricultural production. Through the use of a climate data record (AVHRR NDVI) and modeled temperature and humidity models, we have been able to identify regions that have shown to be sensitive to climate variability during the past two and a half decades. These regions should focus on reducing their vulnerability to climate fluctuations through investments in infrastructure such as irrigation and flexible cropping systems, and in safety nets such as index insurance (Brown et al., 2011) and other forms of government income support for the most vulnerable (Moseley et al., 2010). More analysis can be done that will enable improved targeting of climate adaptation investments to strengthen the global agricultural system.

References

Berg, A. A., Famiglietti, J. S., Walker, J. P., & Houser, P. R. (2003). Impact of bias correction to reanalysis products on simulations of North American soil moisture and hydrological fluxes. *Journal of Geophysical Research*, *108*, 4490.

Brown, M. E., & de Beurs, K. (2008). Evaluation of multi-sensor semi-arid crop season parameters based on NDVI and rainfall. *Remote Sensing of Environment*, *112*, 2261–2271.

Brown, M. E., de Beurs, K., & Vrieling, A. (2010). The response of African land surface phenology to large scale climate oscillations. *Remote Sensing of Environment*, *114*, 2286–2296.

Brown, M. E., Hintermann, B., & Higgins, N. (2009). Markets, climate change and food security in West Africa. *Environmental Science & Technology*, *43*, 8016–8020.

Brown, M. E., Osgood, D. E., & Carriquiry, M. A. (2011). Science-based insurance. *Nature Geoscience*, *4*, 213–214.

Brown, M. E., Pinzon, J. E., Didan, K., Morisette, J. T., & Tucker, C. J. (2006). Evaluation of the consistency of long-term NDVI time series derived from AVHRR, SPOT-Vegetation, SeaWIFS, MODIS and LandSAT ETM+. *IEEE Transactions on Geoscience and Remote Sensing*, *44*, 1787–1793.

de Beurs, K. M., & Henebry, G. M. (2004). Land surface phenology, climatic variation, and institutional change: Analyzing agricultural land cover change in Kazakhstan. *Remote Sensing of Environment*, *89*, 497–509 (doi:410.1016/j.rse.2003.1011.1006).

de Beurs, K. M., & Henebry, G. M. (2008). Spatio-temporal statistical methods for modeling land surface phenology. In I. L. Hudson, & M. R. Keatley (Eds.), *Phenological research: Methods for environmental and climate change analysis*. Springer Verlag.

de Beurs, K. M., & Henebry, G. M. (2010). A land surface phenology assessment of the northern polar regions using MODIS reflectance time series. *Canadian Journal of Remote Sensing*, *36*, S86–S110.

Fang, H. (2009). *README document for the Global Land Data Assimilation System Version 1 Products* (pp. 34). Greenbelt, MD: Goddard Earth System Sciences Data and Information Services Center (GES DISC).

FAO (2011). *FAO Statistical Database*. : Food and Agricultural Organization of the United Nations (FAO).

Funk, C., & Brown, M. E. (2009). Declining Global Per Capita Agricultural Production and Warming Oceans Threaten Food Security. *Food Security Journal*, *1*, 271–289.

Funk, C. C., Dettinger, M. D., Michaelsen, J. C., Verdin, J. P., Brown, M. E., Barlow, M., & Hoell, A. (2008). The Warm Ocean Dry Africa dipole threatens food insecure Africa, but could be mitigated by agricultural development. *Proceedings of the National Academy of Sciences*, *105*(32), 11081–11086.

Graaff, M. A. D., Groenigen, K. J. V., Six, J., Hungate, B., & Kessel, C. V. (2006). Interactions between plant growth and soil nutrient cycling under elevated CO2: a meta-analysis. *Global Change Biology*, *12*.

Hicke, J. A., Asner, G. P., Randerson, J. T., Tucker, C., Los, S., Birdsey, R., et al. (2002). Satellite-derived increases in net primary productivity across North America, 1982–1998. *Geophysical Research Letters*, *29*.

Holben, B. (1986). Characteristics of Maximum-Value Composite Images from Temporal AVHRR Data. *International Journal of Remote Sensing*, *7*, 1417–1434.

Hung, J. H. M., O'Neill, R. T., Bauer, P., & Kohne, K. (1997). The behavior of the P-Value when the alternative hypothesis is true. *Biometrics*, *53*, 11–12.

IAASTD (2008). *International Assessment Of Agricultural Knowledge, Science And Technology For Development*. London: Island Press.

Idso, S. B. (1981). A set of equations for full spectrum and 8- to 14 micrometer and 10.5- to 12.5 micrometer thermal radiation from cloudless skies. *Water Resources Research*, *17*, 295–304.

IPCC (2007). *The Effects of Climate Change on Agriculture, Land Resources, Water Resources and Biodiversity* (pp. 243). Washington DC: Intergovernmental Panel on Climate Change.

Jarlan, L., Tourre, Y. M., Mougin, E., Phillippon, N., & Mazzega, P. (2005). Dominant patterns in AVHRR NDVI interannual variability over the Sahel and linkages with key climate signals (1982–2003). *Geophysical Research Letters*, *32*, L04701.

Jeong, S. J., Ho, C. H., Brown, M. E., Kug, J. S., & Piao, S. (2010). Browning in desert boundaries in Asia in recent decades. *Journal of Geophysical Research-Atmospheres*, *116*, D02103.

Kidwell, K. B. (1998). *Polar Orbiter Data Users' Guide (TIROS-N, NOAA-6, NOAA-7, NOAA-8, NOAA-9, NOAA-10, NOAA-11, NOAA-12, NOAA-14)*. Washington D.C.: National Oceanic and Atmospheric Administration.

Kidwell, K. B. (2000). NOAA KLM Users' Guide. *National Oceanic and Atmospheric Administration*.

Kumar, S. V., Peters-Lidard, C. D., Tian, Y., Houser, P. R., Geiger, J., Olden, S., et al. (2006). Land Information System - An interoperable framework for high resolution land surface modeling. *Environmental Modeling and Software*, *21*, 1402–1415.

Lamb, R. L. (2000). Food crops, exports, and the short-run policy response of agriculture in Africa. *Agricultural Economics*, *22*, 271–298.

Liebmann, B., & Marengo, J. A. (2001). Interannual Variability of the Rainy Season and Rainfall in the Brazilian Amazon Basin. *Journal of Climate*, *14*, 4308–4318.

Lobell, D. B., Schlenker, W., & Costa-Roberts, J. (2011). Climate Trends and Global Crop Production since 1980. *Science*.

Monfreda, C., Ramankutty, N., & Foley, J. A. (2008). Farming the planet: 2. Geographic distribution of crop areas, yields, physiological types, and net primary production in the year 2000. *Global Biogeochemical Cycles*, *22*.

Moseley, W. G., Carney, J., & Becker, L. (2010). Neoliberal policy, rural livelihoods, and urban food security in West Africa: A comparative study of The Gambia, Côte d'Ivoire, and Mali. *Proceedings of the National Academy of Sciences*, *29*, 5–19.

NASS (2012). *National Agriculture and Statistics Service Database*. Washington DC: US Department of Agriculture.

Nemani, R. R., Keeling, C. D., Hashimoto, H., Jolly, W. M., Piper, S. C., Tucker, C. J., et al. (2003). Climate-driven increases in global terrestrial net primary production from 1982 to 1999. *Science*, *300*, 1560–1563.

Nicholson, S. (2005). On the question of the "recovery" of the rains in the West African Sahel. *Journal of Arid Environments*, *63*, 615–641.

Piao, S. L., Fang, J. Y., & Chen, A. P. (2003). Seasonal dynamics of terrestrial net primary production in response to climate changes in China. *Acta Botanica Sinica*, *45*, 269–275.

Piao, S., Fang, J., Zhou, L., Ciais, P., & Zhu, B. (2006). Variations in satellite-derived phenology in China's temperate vegetation. *Global Change Biology*, *12*, 672–685.

Piao, S., Friedlingstein, P., Ciais, P., Viovy, N., & Demarty, J. (2007). Growing season extension and its impact on terrestrial carbon cycle in the Northern Hemisphere over the past 2 decades. *Global Biogeochemical Cycles*, *21*, GB3018.

Schmidhuber, J., & Tubiello, F. N. (2007). Global food security under climate change. *Proceedings of the National Academy of Sciences*, *104*, 19703–19708.

Shapiro, R. (1987). *A simple model for the calculation of the flux of direct and diffuse solar radiation through the atmosphere* (pp. 40). Hanscom AFB, MA: Air Force Geophysics Lab.

Simelton, E., Fraser, E. D. G., Termansen, M., Forster, P. M., & Dougill, A. J. (2009). Typologies of crop-drought vulnerability: an empirical analysis of the socio-economic factors that influence the sensitivity and resilience to drought of three major food crops in China (1961–2001). *Environmental Science & Policy*, *12*, 438–452.

Slayback, D. A., Pinzon, J. E., Los, S. O., & Tucker, C. J. (2003). Northern hemisphere photosynthetic trends 1982–99. *Global Change Biology*, *9*, 1–15.

Storey, J. D., & Tibshirani, R. (2003). Statistical significance for genomewide studies. *Proceedings of the National Academy of Sciences*, *100*, 9440–9445.

Tucker, C. J., Pinzon, J. E., Brown, M. E., Slayback, D., Pak, E. W., Mahoney, R., et al. (2005). An extended AVHRR 8-km NDVI data set compatible with MODIS and SPOT vegetation NDVI Data. *International Journal of Remote Sensing*, *26*, 4485–4498.

White, M. A., de Beurs, K., Didan, K., Inouye, D., Richardson, A., Jensen, O., et al. (2009). Intercomparison, interpretation and assessment of spring phenology in North America estimated from remote sensing for 1982 to 2006. *Global Change Biology*, *15*, 2335–2359.

White, M. A., Thornton, P. E., & Running, S. W. (1997). A continental phenology model for monitoring vegetation responses to interannual climatic variability. *Global Biogeochemical Cycles*, *11*, 217–234.

Zhao, M., & Running, S. W. (2010). Drought-induced reduction in global terrestrial net primary production from 2000 through 2009. *Science*, *329*, 940–943.

Zhou, L., Kaufmann, R. K., Tian, Y., Myneni, R. B., & Tucker, C. J. (2003). Relation between interannual variations in satellite measures of northern forest greenness and climate between 1982 and 1999. *Journal of Geophysical Research-Atmospheres*, *108*.